EAI Endorsed Transactions
on Energy Web

Research Article EAI.EU

Frequency control of power system with electric vehicles using hybrid african vultures optimization algorithm and pattern search tuned fuzzy PID controller

P.M. Dash[1], A.K. Baliarsingh[2] and S.K. Mohapatra[3, *]

[1]Department of Electrical Engineering, BEC, Bhubaneswar, Odisha, India
[2]Department of Electrical Engineering, Government College of Engineering, Kalahandi, Odisha, India
[3*]Department of Electrical Engineering, Government College of Engineering, Keonjhar, Odisha, India

Abstract

In this study, a hybrid African Vultures Optimisation Algorithm (AVOA) and Pattern search (hAVOA-PS) based Fuzzy PID (FPID) structure is proposed for frequency control of a nonlinear power system with Electric Vehicles (EVs). To demonstrate the superiority of the proposed hAVOA-PS algorithm, PI controllers are initially taken into consideration and the results are compared with AVOA, Genetic Algorithm (GA), and Particle Swarm Optimization (PSO) techniques. The PID and FPID controllers are taken into consideration to further improve the dynamic performance. It is evident that FPID controllers dominate PID and PI controllers. In the next step, EVs are included in the test system and a comparative analysis of hAVOA-PS based PI/PID/FPID and FPID+EV is presented. To demonstrate the superiority of the anticipated frequency control scheme for maintaining the system stability under various disturbance conditions, such as load increase in area-1 only, load decrease/increase in all areas, and large load increase in all areas are considered. The proposed hAVOA-PS based FPID controller in the presence of EV is seen to be able to maintain system stability for all cases considered, whereas other compared approaches fail to maintain stability in some cases.

Keywords: African Vultures Optimization Algorithm, Automatic Generation Control, Fuzzy PID Controller, Electric Vehicles, Governor Dead Band, Generation Rate Constraint, Pattern Search.

Received on 24 March 2023, accepted on 23 October 2023, published on 30 October 2023

doi: 10.4108/ew.135

[1]Corresponding author. Email: sangram.muna.76@gmail.com

1. Introduction

In an interconnected power system, unsystematic changes in load cause the tie-line power and frequency deviation to diverge from their rated value. To maintain equilibrium among frequency and generation, an automatic control system is essential. The Automatic Generation Control (AGC) scheme in the power system reduces the frequency and tie-line power deviations by properly varying the generations [1-3]. Many investigators have applied several secondary controllers in the AGC system such as conventional controller, PID controller in AGC of Diesel/Wind turbine generators [4-5], optimal fractional order PID controller was implemented to solve the AGC issue in [6], Bacterial foraging (BF) based integral plus double derivative controller (IDD) and fuzzy IDD controller have been carried out in AGC study [7], two degrees of freedom controller (2DOF) effectively implemented in the multi-microgrid system in [8]. Many advanced controllers such as sliding mode controller utilized in nonlinear systems [9], modified equilibrium optimization tune multistage PID has been carried out in AGC systems [10]. The effect of wind power was also analyzed for AGC studies in [11]. Frequency control for a hybrid distributed power system by tilted PID has been done in [12]. Grasshopper Optimization Algorithm (GOA) tuned multistage PDF+(1+PI) controller has been studied for AGC issues with FACTS in [13]. The impact of various energy storage elements with cascade controllers to mitigate the frequency oscillations has been studied in [14]. To observe the disturbance due to boiler dynamics in the thermal unit and wind power penetration, a Sunflower optimization-based multistage fuzzy controller has been introduced for frequency regulation in [15]. The

impact of H_2 equalizer-based fuel cell in AGC using fuzzy fractional order controller has been introduced in [16].

For solving the AGC problem, optimal tuning of PI controllers with the BAT algorithm has been discussed in [17]. A combined analysis of GA and PSO tuned fuzzy system has been studied in a nonlinear system in [18]. The hybridization of the Multi-verse (MVO) and Pattern Search (PS) technique is employed in the LFC study [19]. Bacteria foraging optimization algorithm based fractional order fuzzy set has been tested for AGC Study in [20]. Hybrid differential evolution (DE)-PSO algorithm is applied to set fuzzy variables in AGC study in [21]. The design and application of the PID controller have been analyzed for real type validation in [22]. The concept of fuzzy logic controllers (FLCs) with energy storage has been implemented in the AGC study in [23]. Frequency control of a practical power system with different types of generation has been studied in [24]. The rule base fuzzy controller is studied in [25]. The PID controller with an adaptive fuzzy structure has been carried out to control nonlinear processes in [26-27].

Recently, novel optimization approaches have been applied for many controller design problems for frequency control. A Prairie Dog Optimization Algorithm has been recently proposed in [28] and its performance is compared with other well-known algorithms using benchmark test functions and some engineering design problems. Dwarf Mongoose Optimization Algorithm (DMO) is proposed in [29] to solve the classical and CEC 2020 benchmark functions and some engineering optimization problems. A Gazelle Optimization Algorithm (GOA) has been proposed and tested using benchmark optimization test functions and selected engineering design problems in [30].

An adaptive hybrid dandelion optimizer by combining three strategies of adaptive tent chaotic mapping, differential evolution (DE) strategy, and adaptive t-distribution perturbation is proposed in [31] to overcome the shortcomings of original dandelion optimizer. A global best-guided firefly algorithm for engineering problems has been proposed in [32]. A Quasi oppositional Jaya tuned two-degree of freedom PID has been projected of a two-area system including the nonlinearities in [33]. A sine logistic map based chaotic sine cosine algorithm tuned PID for frequency regulation of a microgrid with PV, wind, Fuel Cell, BESS, FESS, DEG and MT [34]. A 2DOF-tilted integral derivative with filter tuned by bat and harmony search algorithm has been proposed for two-area wind-hydro-diesel units with SMES and FACTS devices [35]. In [36], a PDF-PI structure tuned by coyote optimization was suggested for frequency regulation of a two-area power system with PV, wind farm & gas turbine interconnection. A Chaotic atom search optimization tuned FOPID structure for frequency control of a hybrid system was presented in [37]. Mayfly optimization tuned Fuzzy PD-(1+I) configuration was recommended in [38] for a microgrid containing Solar–thermal, Wind, Micro-hydro turbine, Biodiesel and Biogas generators. Atom Search Optimization and Grey Wolf Optimization (GWO) based FOPID controllers have been proposed to control frequency of hybrid power system containing PEV, WTPG, STPG and thermal units considering nonlinearities [39, 40].

A. Research Gap & Motivation

The study of recent articles based on AGC problems confirms that various combined efforts of control approaches along with optimizing tools are successfully interfaced with some power grid models to get improved solutions. But no particular approach can give satisfactory results for all types of problems. Therefore, this is an opportunity to explore alternative approaches by suggesting novel robust control schemes.

African Vultures Optimization Algorithm (AVOA) is a lately proposed optimization method inspired by the African vultures' navigation and foraging characteristics [41,44]. The dominance of AVOA over GWO, PSO, FFA, WOA, MFO, TLBO, DE, BBO, GSA, SSA, and IPO has been demonstrated using benchmark test functions. However, the effectiveness of AVOA over other similar techniques in controller design problem has not been reported. Also, as AVOA is a global search technique look at the broad search area and may not be effective if used unaided. On the other hand, Pattern Search (PS) which is a local search method searches the local area but not effective for wider search [8, 19, 21]. In consequence of their strengths, these two methods can be mixed to get improved performance. Therefore, a hybrid AVOA-PS method is projected in this paper for tuning of fuzzy PID (FPID) parameters for frequency control of power system.

The main contribution of this research work to overcome the weakness recognized in the performance of the normal version of the AVOA: local optima trapping and minimal population diversity which results in premature convergence. Because of these lacking AVOA needs to be improvised or hybridized with other techniques or local search optimizations. The improvement in performance is noticed, by hybridizing the normal AVOA and Pattern search (PS) algorithm called hAVOA-PS. The novel contributions of the present study are:

- A new nature-inspired evolutionary hybridized AVOA and PS (hAVOA-PS) is projected for frequency regulation of a five-area nonlinear power system in presence of electric vehicle.
- To justify the supremacy of the projected algorithm (hAVOA-PS), it is related to other conformist techniques like GA, PSO, and AVOA.
- A fuzzy-PID (FPID) controller is designed using hAVOA-PS and the performance of FPID with EV is compared with FPID without EV as well as PID and PI controllers.
- To show the superiority of projected frequency control scheme in maintaining the stability of system under different disturbance conditions like load increase/decrease in all areas and large load increase in all areas.

B. Paper Organization

The research paper is systematized into six major segments. Section I gives the introduction, research gap & motivation, and paper organization. The test system has been described in section II. The control system and objective function are described in section III. Overview of proposed hybrid African Vultures Optimization Algorithm (AVOA) and Pattern search (hAVOA-PS) is given in section IV. Section V deals with the results and analysis of the proposed work by including various operational situations. Lastly, the conclusion of the studied research work is presented by highlighting the major research outcomes.

2. Test System

An interconnected power system consisting of 5 areas is taken as test system as revealed in Fig. 1. The areas are: area-1: thermal-hydro, area-2: thermal-wind, area-3: thermal-gas, area-4: hydro-diesel and area-5: hydro-wind. Dissimilar rating (P_{Ri} and P_{Rj}) of areas i and j, a factor a_{ij} =- P_{Ri}/ P_{Rj}, is employed to characterize the values in p.u. In frequency control studies, it is important to study the elementary physical constraints and take account of them to get an appropriate knowledge of the frequency control issues. The main constraints are Generation Rate Constraint (GRC) and Governor Dead Band (GDB) nonlinearity which are taken as 3%/ min and 0.036 Hz respectively [5]. Also, for the thermal unit's boiler dynamics are included. Model of wind, gas, diesel and hydro units are adopted from literature [42-43]. The information offered by Fosha and Elgerd [1] is referred for developing the system model. The system data are taken from [5, 35, 42-43]. With the growing demand for electric vehicles (EV), it is expected that EVs will be extensively used in future power systems. EVs give a prospect to employ their batteries during plug-in. considering a fleet of EVs, they could act as ancillary facilities for the future power system. It is therefore necessary to evaluate the capability of EVs in frequency control of studied system. The figure presentation modelling of EV for frequency control is demonstrated in Fig. 2 [40]. The LFC signal ΔU is supplied to EV for discharging/charging. Parameters $\pm BkW$ signify the battery capacity. The existing battery energy is signified by E that is kept inside the restrictions $E_{\max}$ and $E_{\min}$ presumed as 90% and 60%. K_1 and K_2 are found as $K_1 = E - E_{\max}$, $K_2 = E - E_{\min}$,. The stored energy part in Fig. 2 computes the remaining stored energy.

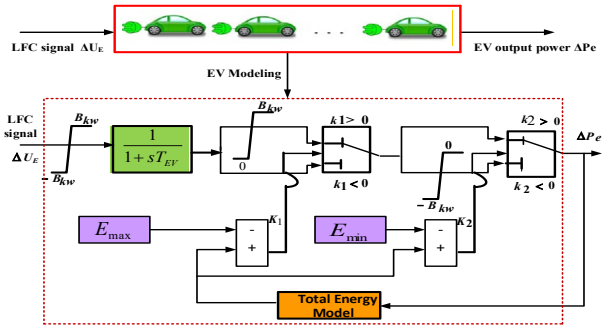

Fig. 2. EV Modelling for frequency control

3. Controller structure and Objective Function

The Proportional Integral (PI) controllers are generally employed in control systems for their modest design, less cost, and their practicality for linear systems. However, traditional PI structures are usually not competent for nonlinear systems. A Fuzzy Logic Control (FLC) based PI (FPI) structure increases the system performance as fuzzy logic can deal with nonlinearity [8, 9]. Design of an appropriate FLC involves choice of appropriate membership functions (MFs) and construction of rules which is a complex task. On the other hand, common rule base and MFs can be selected, and the Scaling Factors (SFs)/PI parameters can be optimized for satisfactory operation [23, 24]. Nevertheless, the FPI configuration might yield unacceptable system performance in initial periods for nonlinear systems due to its intrinsic integral act. To overcome this, a derivative component is added resulting in Fuzzy PID (FPID) controller [25, 26]. Therefore, a FPID controller revealed in Fig. 3is selected in this study for frequency control. Individual Area Control Errors (ACE) and their derivatives are passed through SFs (K_I and K_2) and given as inputs to FPID. The FLC output is passed through a PID controller where K_P, K_I and K_D are the PID parameters. The FPID outputs manage the powers of specific generating units.

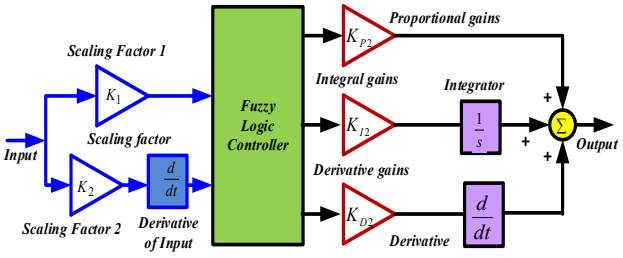

Fig. 3. Fuzzy PID configuration

3.1 Fuzzy Logic Controller Design

Usually triangular (MFs)are favoured as its real-world

execution can simply be attained. It also requires lowest storage obligation and can be functioned economically to meet the stiff real time necessities. Same MFs for inputs/output is typically preferred from computational adeptness viewpoint in addition to memory management ability [26]. Thus, similar MFs are chosen for the inputs/output of FLC. The linguistics Large Negative (LN), Small Negative (SN), Zero (Z), Small Positive (SP) and Large Positive (LP) are used as illustrated in Fig. 4.

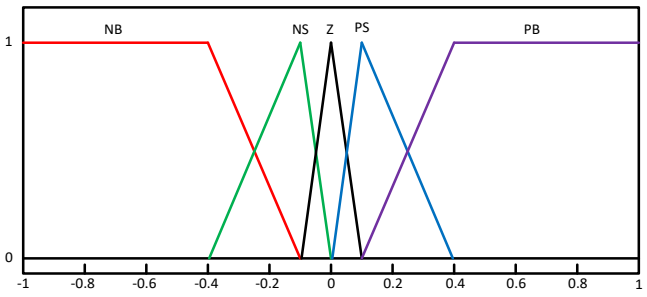

Fig.4. MFs of error and change of error of CFPID

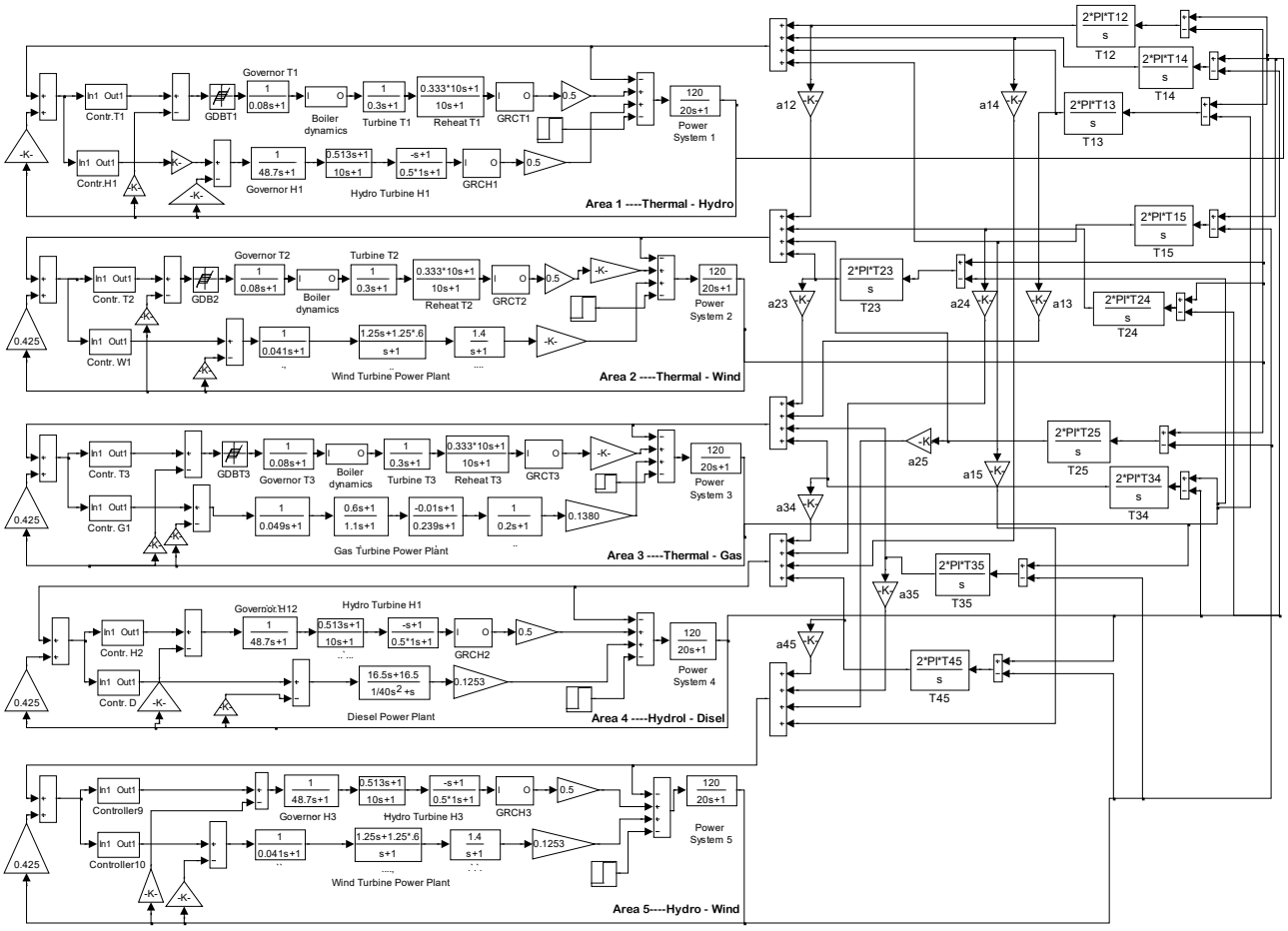

Fig. 1. Five area ten-unit system under investigation

Mamdani and centre of gravity methods are selected as fuzzy interface engine and defuzzification method. The rule base is shown in Table 2. An ITAE criteria specified in Eq. (1) is selected as it yields minimum Over Shoots (OS) and settling times related to other measure like ISE, IAE, ITSE and ISTE.

$$J = ITAE = \int_0^t \left(\left| \Delta F_i \right| + \left| \Delta P_{Tie-i} \right| \right) \cdot t \cdot dt \qquad (1)$$

where, ΔF_i and ΔP_{Tie-i} are frequency and tie-line power deviation in i^{th} area and t is simulation time.

Table 1: Rule base for error, derivative of error and FLC output

de/dt / e	LN	SN	Z	SP	LP
LN	LN	LN	SN	SN	Z
SN	LN	SN	SN	Z	SP
Z	SN	SN	Z	SP	SP
SP	SN	Z	SP	SP	LP
LP	Z	SP	SP	LP	LP

4. Hybrid African Vultures Optimization Algorithm and Pattern Search

4.1. African Vulture Optimization Algorithm (AVOA)

AVOA is a new population-based search algorithm proposed in year 2021 [36]. The algorithm is motivated by way of life, food explore and struggle for food by different vultures in Africa. In AVOA, a balance between diversity and quality is formed by the employing two best solutions in AVOA. The four stages AVOA algorithms are:

(i). Finding the best vulture: 1st Stage

After initialization, the fitness of every candidate is found, and the first- and second-best solutions are chosen as the two best candidates. The remaining candidates shift toward these best solutions as per Eq. (2)

$$R(i)=\begin{Bmatrix} Best\ Vulture_1 & if\ p_i = L_1 \\ Best\ Vulture_2 & if\ p_i = L_2 \end{Bmatrix} \quad (2)$$

In Eq. (2), the probability of selecting the particular vultures is determined using Eq. (3) i.e., Roulette wheel, where L_1 and L_2varies between 0 and 1 and their sum is 1. If one parameter is close to 1 and then the other parameter will be close to 0 causing increased intensification. The reverse values result in increased diversification.

$$pi=\frac{F_i}{\sum_{i=1}^{n} F_i} \quad (3)$$

b. Starvation rate of vultures: 2nd Stage

Vultures look out for food at all times and have a sufficient energy when they're satiated, allowing them to look for food at larger distances, but when they're hungry, they don't have the energy to fly. This is mathematically expressed in Eq. (4).

$$F=\left(2\times rand_1+1\right)\times z\times\left(1-\frac{IT_i}{IT_M}\right)+t \quad (4)$$

Where

$$t=h\times\left(sin\left(\frac{\pi}{2}\times\frac{IT_i}{IT_M}\right)^{\gamma}+cos\left(\frac{\pi}{2}\times\frac{IT_i}{IT_M}\right)-1\right) \quad (5)$$

In above Eqs., F signifies the satisfactions, IT and IT_Ms indicate the current & max iterations; $rand_1$, z and h are arbitrary values between (0 to 1), (-1 to 1) and (-2 to 2). When the z value falls below zero, the vulture is starving; when it increases to zero, the vulture is satiated. There is no assurance that the finishing solutions will contain correct approximations of the global best at the conclusion of the exploration stage when addressing difficult optimization issues. As a result, it results in an early convergence at the best local site. Eq. (4) is utilized to improve effectiveness while solving difficult optimization tasks, which results in a higher degree of dependability for escape from local optimal spots. The AVOA algorithm's final iterations execute the exploitation stage and, in some cases, exploration activities. The overall objective of this technique is to adjust Eq. (5) to switch among the exploration and exploitation stages, hence increasing the chance of the AVOA algorithm performing the exploration stage sometime during the search procedure. In Eq. (4), 'sin' and 'cos' denote the sine and cosine functions, respectively. The parameter 'w' is a fixed value set prior to the search process that specifies whether the search process disturbs the exploration and operation stages; increasing the 'w' parameter enhances the probability of performing the exploration stage in the later search process.

The total number of vultures is decreasing, and the rate of decline is increasing with each repeat. When |F| exceeds 1, vultures begin hunting for food in new sites, initiating the exploration phase of the AVOA. If |F| <1, AVOA initiates the exploitation stage, during which vultures begin seeking food in nearby areas.

c. Exploration: 3rd Stage

In this stage, the vultures have extraordinary vision and an incredible capability to seek food and identify dead animals in their native habitat. Vultures, on the other hand, occasionally face food shortages. Vultures spend considerable time inspecting their surroundings and cover enormous path in search of food. Vultures can use one of two separate techniques to investigate different random sites inside the AVOA, and a factor called P_1 is employed for selecting which scheme to apply. This parameter has a worth between 0 and 1, influencing how each of the scheme is followed.

To choose any of the schemes in the $rand_{P1,}$ exploration stage, an arbitrary value between 0 and 1 is created. The vulture location in next iteration is calculated as:

$$P(i+1)=\begin{Bmatrix} Equation(7) & if\ p_i \geq rand_{P1} \\ Equation(9) & if\ p_i < rand_{P1} \end{Bmatrix} \quad (6)$$

$$P(i+1)=R(i)-D(i)\times F \quad (7)$$

$$D(i)=\left|X\times R-D(i)-P(i)\right| \quad (8)$$

In Eq. (7), Vultures arbitrarily look for food in the nearby region within a haphazard distance of one of the two groups' greatest cultures. In above Eqs., $P(i)$ and $P\,(i+1)$ are the vulture location vector in the present & next iterations and F is the vulture satiation rate in the present iteration; R(i) is one best vulture, as determined by the current iteration's usage of Eq. (2). Additionally, X is the location of vultures that fly randomly in order to guard food from several vultures and is found by $X = 2 \times rand$, where rand is an arbitrary value between 0 and 1. $P(i)$ is the present vector location of the vulture.

$$P(i+1)=R(i)-F+rand_2\times\left(\left(ub-lb\right)\times rand_3+lb\right) \quad (9)$$

Where $rand_2$ and $rand_3$ are random values in the limit 0 and 1, lb and ub are the bound of the variables.

d. Exploitation: 4the Stage

In this stage, if $|F|<1$, the AVOA performs exploitation in two phases with different schemes. The factor $P_2$and P_3 are employed to choose the schemes available in the first and second stage. Both $P_2$and P_3lie between 0 and 1.

Exploitation: The algorithm performs the first step in the Exploitation stage if $|F|$ lies among 1 and 0.5. Here, two diverse rotating flight and siege-fight schemes are executed as given in Eq. (10):

$$P(i+1)=\begin{Bmatrix} Equation(11) & if\ p_i \geq rand_{P2} \\ Equation(14) & if\ p_i < rand_{P2} \end{Bmatrix} \quad (10)$$

Competition for Food: If $|F|=0.5$, vultures are reasonably satisfied and have an enough supply of energy. When a large number of vultures concentrate around a single food supply, serious fights over food acquisition can occur. At such situations, physically powerful vultures do not wish to share the food, but the weaker ones attempt to exhaust the strong vultures and get food from them by congregating around robust vultures and instigating trivial fights. This is replicated using Eqn. (11) and (12).

$$P(i+1)=D(i)\times(F+rand_4)-d(t) \quad (11)$$

$$d(t)=R(i)-P(i) \quad (12)$$

$D(i)$ is evaluated by Eq. (8), $rand_4$ is a four-digit arbitrary value between 0 and 1

Vultures rotating flight: Vultures are known for their rotating flying representing spiral movement. In this procedure, a spiral expression is generated among all vultures. Eqs. (12) and (13) are used to express circular flight (13).

$$S_1=R(i)\times\left(\frac{rand_5\times P(i)}{2\pi}\right)\times cos\left(P(i)\right) \quad (13)$$

$$S_2=R(i)\times\left(\frac{rand_6\times P(i)}{2\pi}\right)\times sin\left(P(i)\right) \quad (14)$$

$$P(i+1)=R(i)-(S_1+S_2) \quad (15)$$

R(i) indicates the location vector of one best vulture in the present iteration. And $rand_5$ and $rand_6$ are random numbers ranging from 0 to 1. Here S1 and S2 are calculated using Eq (13). Finally, the position of the vultures is reorganized using Eq. (14).

e. 2nd Exploitation Stage: In this stage, if $|F| < 0.5$, the two vultures' travels gather some more vultures near food, and the blockade and hostile conflict to locate food are performed. This process is revealed as

$$P(i+1)=\begin{Bmatrix} Equation(17) & if\ p_3 \geq rand_{P3} \\ Equation(18) & if\ p_3 < rand_{P3} \end{Bmatrix}$$

Gathering of vultures near food: Sometimes**,** vultures are hungry, several vultures gather near the food. This process is revealed as:

$$A_1=Best\ Vulture_1(i)-\frac{Best\ Vulture_1(i)\times P(i)}{Best\ Vulture_1(i)-P(i)^2}\times F$$

$$A_1=Best\ Vulture_1(i)-\frac{Best\ Vulture_1(i)\times P(i)}{Best\ Vulture_1(i)-P(i)^2}\times F \quad (16)$$

In Eq. (16), $BestVulture1(i)$ and $BestVulture2(i)$are the best vulture of the 1st and 2ndgroup in the present iteration.

At last, the aggregation of all vultures is carried out by:

$$P(i+1)=\frac{A_1+A_2}{2} \quad (17)$$

Hostile rivalry for Food: When $|F|$ <0.5, the leader vultures is starved and frail and don't have adequate power to handle other vultures. The vultures move towards the leader vulture as:

$$P(i+1)=R(i)\left|d(t)\right|\times F\times Levy(d) \quad (18)$$

When d(t) is used in Eq. (17), it reflects the space among a vulture and one best vulture in each of the 2 groups, which is determined using Eq (12). Eq. (18) has been improved by employing Levy flight (LF) patterns LF patterns have been found and exploited in the actions of several search processes, and they have been used to improve the efficacy of the AVOA. The LFs were determined with the help of Eq. (19).

$$LF(x)=0.01\times\frac{u+\sigma}{|v|^{\frac{1}{\beta}}},\ \sigma=\left(\frac{\Gamma(1+\beta)\times sin\left(\frac{\pi\beta}{2}\right)}{\Gamma(1+\beta_2)\times\beta\times 2\left(\frac{\beta-1}{2}\right)}\right)^{\frac{1}{\beta}} \quad (19)$$

Equation (19) denotes the problem dimensions, where d indicates the size of the problem, u and v denote random numbers between zero and one and denotes a fixed and default value of 1.5.

4.2. Pattern Search (PS)Algorithm

For solving nonlinear optimization problem, pattern search (PS) algorithm is a powerful tool to obtained local optima from a global solution. The initial value of PS algorithms starts with M_0, this initial value is provided by the MFO algorithm. In the first iteration, the patterns are created in the form of [0 1], [1 0], [−1 0] and [0 −1], a lattice point is formed by considering the preliminary point M_0 as M_0 + [0 1], M_0 + [1 0], M_0 + [−1 0], and M_0 + [0 −1]. The performance index is measured until it grasps a lesser value than the preliminary value of M_0. This point is termed M_1 which is the preliminary point for the subsequent iteration. Therefore, at the next recapitulation the lattice point converts: M_1 + 2 * [0 1], M_1 + 2 * [1 0], M_1 + 2 * [−1 0], and M_1 + 2 * [0 −1], and this procedure is progresses till the ending criteria is attained. If not satisfied the initial point can be taken by multiplying a factor of 0.5 known as the contrast factor. So that the lesser performance index is attained, and this progression will be recurrent till the end criteria are accomplished.

Pseudo-code of AVOA

Initialization

Initialize the population size N and maximum iterations T

Initialize the positions of all vultures Pi (i = 1, 2,..., N)

Initialize controlling parameters P_1, P_2, P_3, and w

While t < Tdo
Calculate the vultures' fitness values
Find the first- and second-best positions of vultures $P_{BestVulture1}$ and $P_{BestVulture2}$
for each vulture **do**
Calculate F using Equation (4)
Determine $R(i)$ using Equation (2)
if $|F| \geq 1$ **then**
if P1≥rand P1 **then**
Update vulture' position using Equation (7)
else
Update vulture' position using Equation (9)
end if
else
if $|F| \geq 0.5$ **then**
ifP2≥randP2 **then**
Update vulture' position using Equation (11)
else
Update vulture' position using Equation (15)
end if
if P3≥randP3 **then**
Update vulture' position using Equation (17)
else
Update vulture' position using Equation (18)
end if
end if
end if
end for
end while
Return the first best vulture

PS algorithm

Step-1: Initialize the input parameters for pattern search algorithm
i.e. acceleration factor(v), perturbation vector (P^0) and perturbation tolerance vector (τ)
Step-2: initialize the current perturbation vector $P \leftarrow P^0$ and select the value for the starting point x^{int}
Step-3: Update x^{int} to x^{iter} using exploratory search around x^{int} to find an improved point x^{iter} that has a better value of objective function
if $x^{iter} > x^{int}$
DO $P \leftarrow P/2$
if $P_i < \tau$
DO $x^{iter} = x^{int}$
else
Go to step-3 and update the solution vector using exploratory move
else
DO $x^{final} = x^{int}$, $P \leftarrow P^0$ and go to step-4
end
end

Step-4: Apply pattern move using following steps:
Step-4(a) obtain tentative x^{iter+1} by a pattern move from x^{int} through x^{iter}
Step-4(b) Obtain final x^{iter+1} by an exploratory search around tentative x^{iter+1}
if $f(x^{iter+1}) > f(x^{iter})$
DO $x^{int} \leftarrow x^{iter}$ *and go to* step-3
else
DO $x^{int} \leftarrow x^{iter}$, $x^{iter} \leftarrow x^{iter+1}$ *and go to* step-4
end

5. Results and Discussions

A. Application of hAVOA-PS Algorithm

At first, PI controllers are assumed in every area. All the controller values are selected in the limit [-2 to 2]. The system data are taken from reference [5, 25]. The test system is simulated by applying a different Step Load Increase (SLI) in all areas. To validate the superior performance of hAVOA-PS technique, the PI values are optimized by hAVOA-PS, AVOA, PSO and GA methods. The algorithms parameters are given in Table 2. For all the methods, 30 no. of search agents and 100 iterations (90 for AVOA and 10 for PS) are taken and each method is run 30 times. The optimal results (as per least *ITAE* value) obtained in 30 runs are used as the controller parameters. The optimal PI controller parameters are presented in Table 3. The reported data in Table 3 indicate that the hAVOA-PS optimization method gives the most excellent result. It is clear from Table 3 that for same PI structure, less *ITAE* value is attained with AVOA (*ITAE*= 94.3648) related to GA (*ITAE*=117.5836) and PSO (*ITAE*= 106.9478). The *ITAE* value is reduced to 71.6407when hAVOAO-PS is engaged. The % reduction in *ITAE* value with hAVOAO-PS method related to GA, PSO, and AVOA are 39.07%, 33.01% and 24.08% respectively. This authenticates that hAVOAO-PS is superior to AVOA, GA and PSO.

In the next stage, PID and FPID controllers are considered and EVs are included in the system model. The controller values are given in Table 4. It can be seen from Table 4 that the *ITAE*values are progressively decreased with PID, FPID and FPID with EV.
To measure the controller performance, the following cases are assumed:
Case 1: Different SLI in all areas
Case 2: Different Step Load Decrease (SLD) in all areas
Case 3: SLI in some areas and SLD in some areas
Case 4: Large SLIs in all areas

Table 2: Parameter setting of GA, PSO, AVOA & PS algorithms

Method	Values	Description
GA	Tournament	Selection
	0.9 and 0.1	Crossover and mutation rates
PSO	Reduces from 0.9 to 0.2	Inertia weight, w
	2	Social & Cognitive components, c_1 &c_2
AVOA	0.6, 0.4, 0.6	Probability parameters p_1, p_2, p_3
	0.8, 0.6, 2.5	Parameters α, β, γ
PS	1	Mesh size
	2 and 0.5	Mesh expansion and contraction factors

Table 3: Optimal PI controller parameters

		GA/PI (K_P, K_I)	PSO/PI (K_P, K_I)	AVOA/PI (K_P, K_I)	hAVOA-PS/PI (K_P, K_I)
Area-1	Thermal	-0.7091,0.1581	-0.8152, 0.1538	-0.1300, 0.4004	-0.8147, 0.5704
	Hydro	-0.0011, -0.0238	-0.0012, -0.0107	-0.0010, -0.0191	-0.0015, -0.0397
Area-2	Thermal	-0.2421, 0.2465	-0.0827, 0.1298	-0.1032, 0.2340	-0.6571, 0.5319
	Wind	-0.2123, -0.2776	-0.2881, -0.1578	-0.1149, -0.1635	-0.3571, -0.3077
Area-3	Thermal	-0.1077, 0.0759	-0.0724, 0.0918	-0.0533, 0.0880	-0.1725, 0.0981
	Gas	-0.0776, 0.1542	-0.1199, 0.1180	-0.0482, 0.0966	-0.1392, 0.2054
Area-4	Hydro	0.0693, 0.3307	0.0762, 0.5363	0.1972, 0.7925	0.2947, 0.8385
	Diesel	0.0759, 0.0574	0.1259, 0.0925	0.1358, 0.4396	0.1786, 0.5048
Area-5	Hydro	0.4786, -0.0317	0.1226, -0.0406	0.5068, -0.0686	0.5193, -0.0779
	Wind	-0.1541, 0.7553	-0.4051, 0.7156	-0.3331, 0.8572	0.4608, 0.9301
ITAE		117.5836	106.9478	94.3648	71.6407
ISE		29.0268	25.8679	24.6891	22.2231
ITSE		211.7059	149.7962	123.3924	90.2133
IAE		678.7248	596.3770	436.0847	374.5142

Case 1:

In this case, 2% SLI in areas 1 &2and 4% SLI in areas 3, 4&5are assumed. The response with PI controller optimizedby different optimization techniques is displayed in Fig. 5. It can be noticedfrom Fig. 5 that, with same PI structure, the performaance with hAVOAO-PSmethod is better than GA, PSO and AVOAmethods. This demonstrates the dominance of hAVOAO-PS over AVOA, PSO and GA.

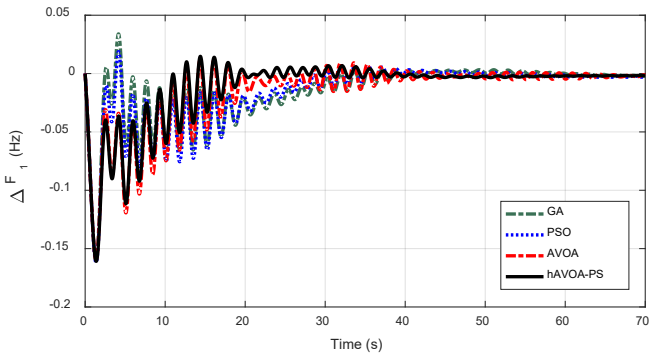

Fig. 5. Case 1: Comparison of techniques with PI controllers

The system dynamic response with PI, PID, FPID and FPID with EV for the above disturbance are shown in Figs. 6 (a)-(f).It is also clear from Figs. 6 (a)-(e) that the responses with FPID conroller with EVprovides enhanced performance related to FPID, PID and PI. It is observed from Tables 3-4 and Figs. 5-6 that the numerical values of ITAE, Overshoots (Os) and Undershoots (Us) due to hAVOAO-PSoptimized FPID+EV are found to be least related to others. It is noticed that with the same hAVOAO-PSmethod, smallest *ITAE* value (*ITAE*= 16.4128) is attained with FPID with EV compared to FPID (*ITAE*= 27.1889) and PID (*ITAE*= 60.1040). The percentage reduction in *ITAE* with FPID+EVrelated to PI, PID, and FPID are 77.09%, 72.69% and 39.63% respectively.

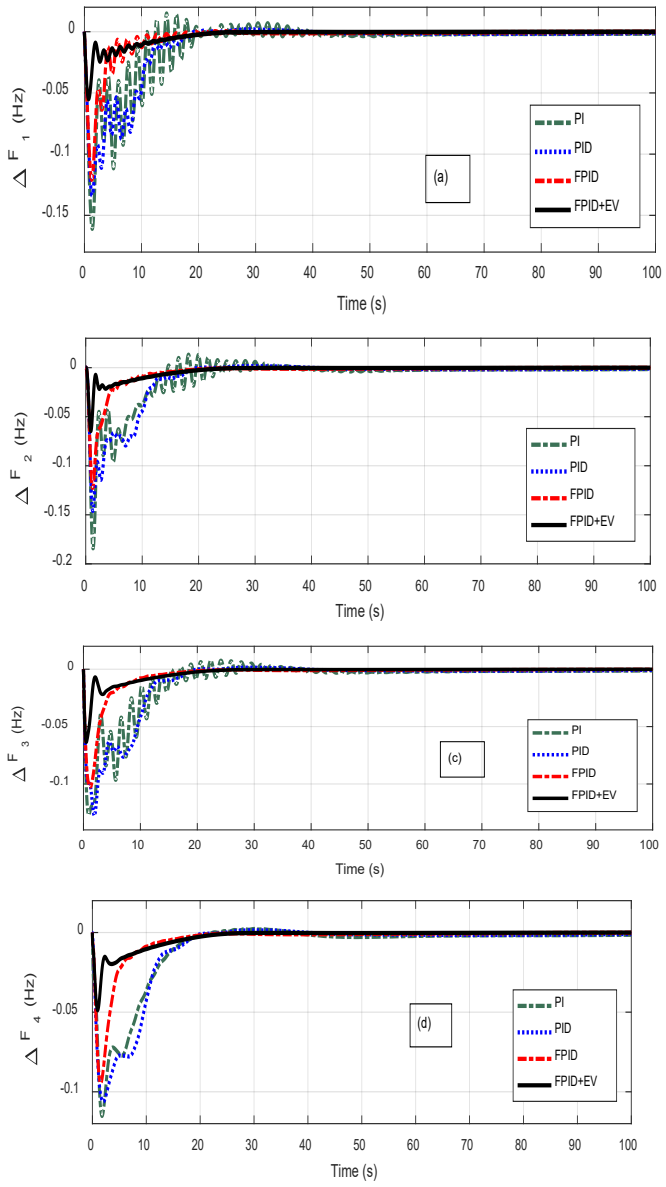

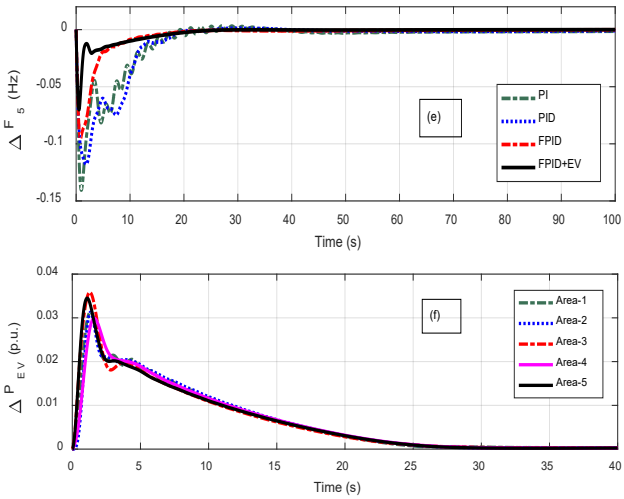

Fig. 6 System response for Case-1

The output powers of EVs connected to each area is shown in Fig. 6 (f) which indicates that, power is supplied by each EVs to meet the SLIs in each area and hence improved response are obtained for the system with FPID+EV.

Case 2:

In this case, 4% SLD in areas 1 & 5 and 3% SLD in areas 2, 3 & 4 are assumed. The system dynamic response with PI, PID, FPID and FPID with EV for the above disturbance are shown in Figs. 7 (a)-(f).It is also obvious from Fig. 7 (a)-(e) that the system with FPID+EV conroller offers improved response than FPID, PID and PI controllers. It is noticed that, for the above case, the *ITAE* value attained with FPID+EVis less (*ITAE*= 31.2846) compared to FPID (*ITAE*= 40.7368), PID (*ITAE*= 107.4927) and PI (*ITAE*= 113.7483). The % reduction in *ITAE* with FPID+EVrelated to PI, PID, and FPID are 72.49%, 70.89% and 23.21% respectively. In this case, as load is decrease in each area, EVs receives power as shown in Fig. 7. (f).

Table 4:hAVOA-PSoptimized controller parameters

		hAVOA-PS/PID (K_P, K_I, K_D)	hAVOA-PS/FPID (K_1, K_2, K_P, K_I, K_D)	hAVOA-PS/FPIDwith EV (K_1, K_2, K_P, K_I, K_D)
Area-1	Thermal	-0.5190, 0.7832, -0.1312	0.5797, 0.6402, -0.5747, -1.5080, -0.2379,	0.6129, 0.4532 -0.3684, -1.4122, -0.0913
	Hydro	-0.0008, -0.0597, 1.6757	0.1383, 0.4728 -1.0494, -0.0082, -1.0835,	0.1068, 0.3997 -1.0253, -0.0060, -0.6771
Area-2	Thermal	-0.2058, 0.1894, 0.6750	0.8951, 0.7342, -1.2764, -1.1513, -0.2893,	0.4152, 0.7042 -1.4002, -0.6211,-0.1285
	Wind	-0.4978, -0.2131, 0.9488	0.5201, 0.1016, -1.5130, -0.2639, -0.6514,	0.4298, 0.0331 -0.8977, -0.3150, -0.5977
Area-3	Thermal	-0.1457, 0.0890, 1.3585	0.8716, 0.5120, -1.6550, -0.3152, -0.3235,	0.4562, 0.4865 -0.7546, -0.3508, -0.3096
	Gas	-0.1670, 0.1781, 1.1276	0.1616, 1.0830 -1.1160, -1.3619, -1.6735,	0.1528, 0.8078 -0.8874, -1.2311, -0.9502
Area-4	Hydro	0.9591, 0.4088, 0.0077	0.4720, 0.7936, -0.3867, -0.3008, -0.6989,	0.4366, 0.3948 -0.4903, -0.1907, -0.4842

Area-5	Diesel	0.2026, 0.9324, 1.4071	0.7425, 0.0149, -1.1468, -0.8772, -0.0128,	0.5278, 0.0182 -1.0943, -0.7534, -0.0130
	Hydro	0.3763, -0.0556, 0.5278	0.0559, 0.6818, -1.5028, -1.2944, -0.7142,	0.0617, 0.7491 -1.9971, -0.8411, -0.3231
	Wind	-0.4483, 0.9333, 1.7773	0.5968, 0.5250, -0.8821, -1.2837, -0.5898,	0.3886, 0.4870 -0.7029, -0.8367, -0.4218
ITAE		60.1040	27.1889	16.4128
ISE		14.9141	6.7972	4.1032
ITSE		108.4910	49.0774	32.8256
IAE		348.6311	158.0750	96.5459

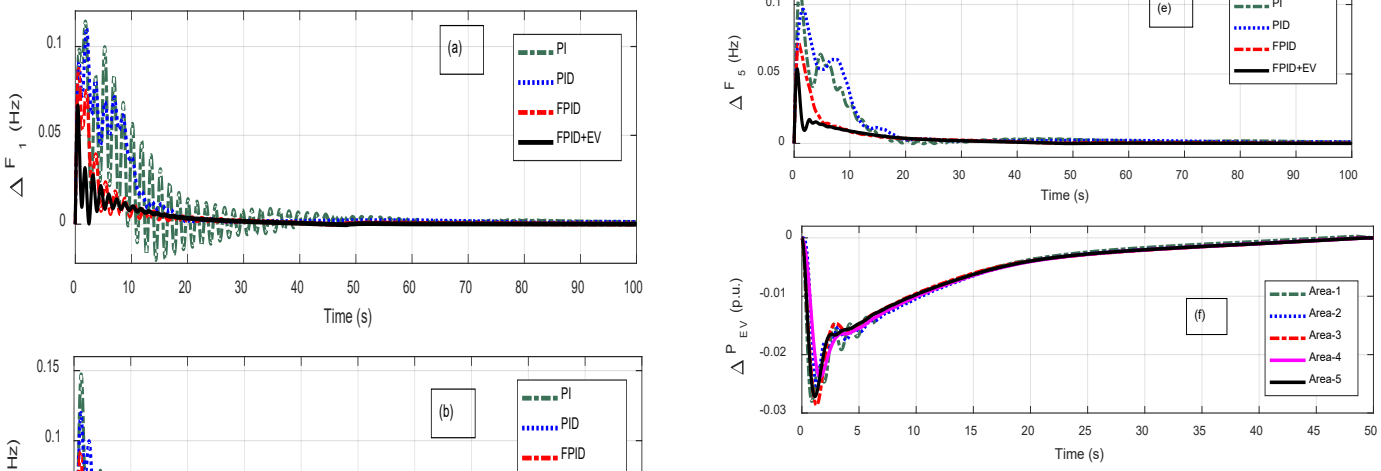

Fig. 7 System response for Case-2

Case 3:

In this case, 1% SLD in areas 1 &2and 3% SLI in areas 3, 4&5are assumed. The system dynamic response with PI, PID, FPID and FPID with EV for the above disturbance are shown in Figs. 8 (a)-(f). It is also evident from Fig. 8 (a)-(e) that, in this case also, the system with FPID+EV provides improved response than FPID, PID and PI.It is noticed that, for the above case, the *ITAE* value attained with FPID+EVis less (*ITAE*= 5.3708) compared to FPID (*ITAE*= 10.1623), PID (*ITAE*= 38.8031) and PI (*ITAE*= 48.1602). The percentage reduction in *ITAE* with FPID+EVrelated to PI, PID, and FPID are 88.84%, 86.15% and 47.14% respectively. The EVs receives/supplies power during the initial periods as per the SLI/SLD in that area as shown in Fig. 8 (f).

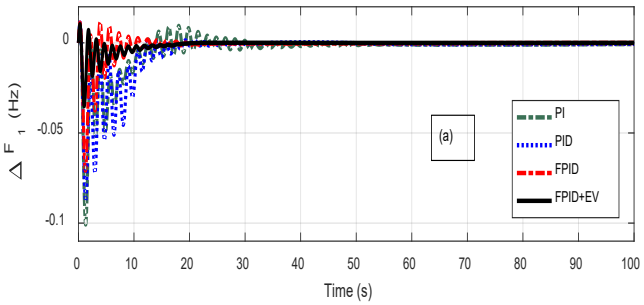

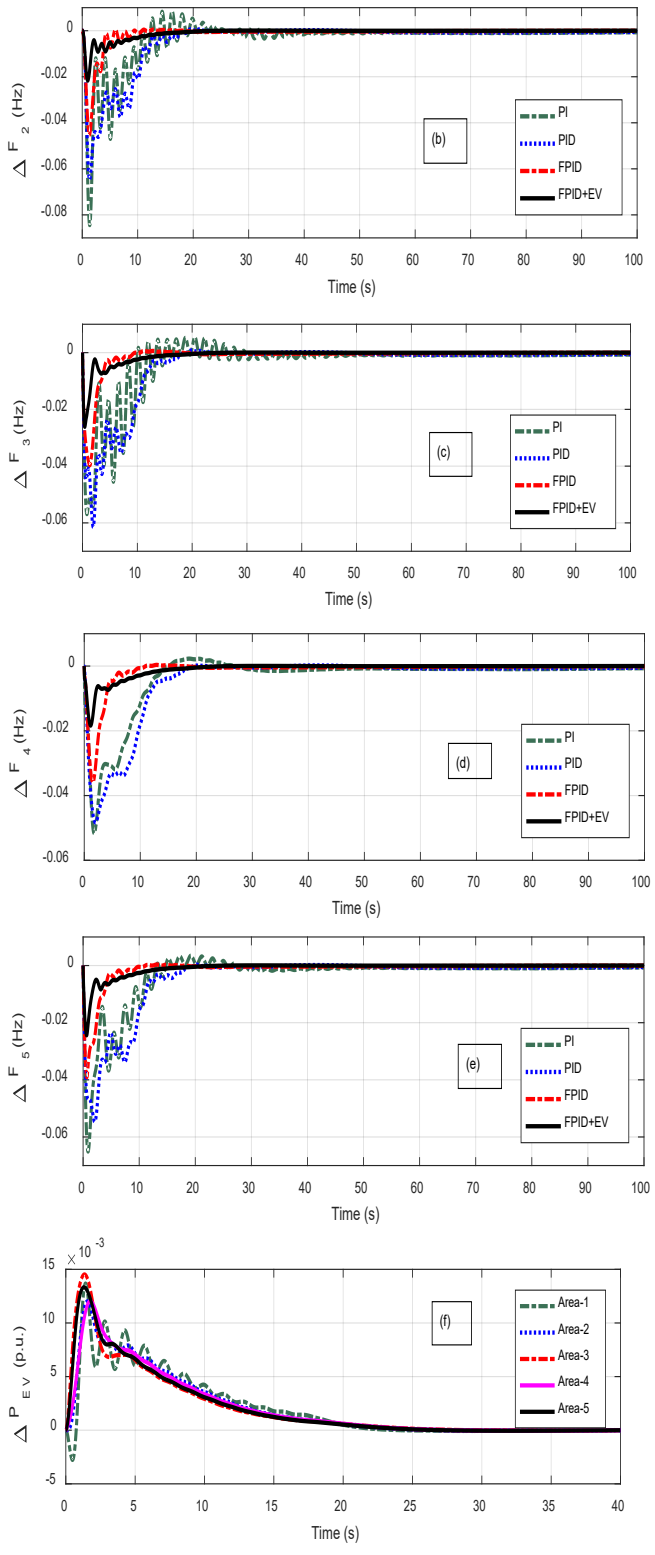

Fig. 8 System response for Case-3

Case 4:

Here, a large SLI of 10% is assumed in all the areas. The system response for the above case are shown in Fig. 9 (a)-(f). It is also evident from Fig. 9 (a)-(e) that the system is unstable with PI and PID for the above case and the system stability is preservedwhen FPID and FPID+EV are implemented. It is also seen that the system response with FPID+EV is better than FPID only. This is because of the real power supplied by the respective EVs during the initial transient period as shown in Fig. 9 (f). Also the ITAE value with FPID+EV is found to be less (ITAE=274.8931) compared to FPID (ITAE=290.7635).

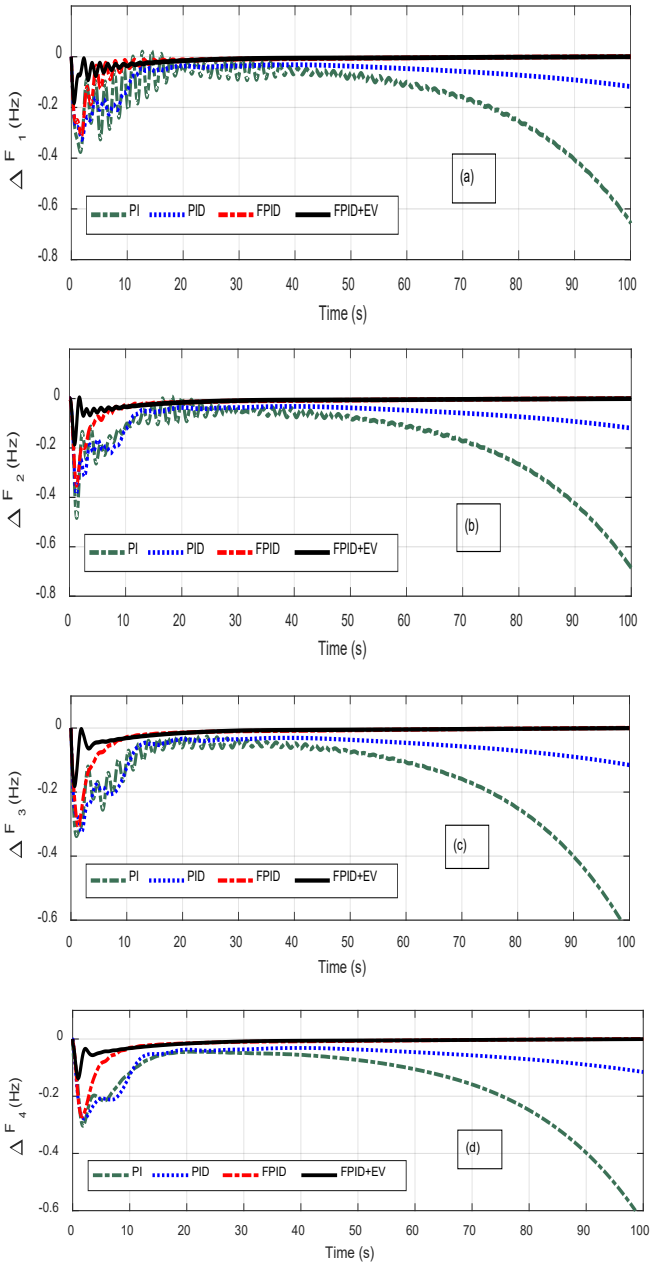

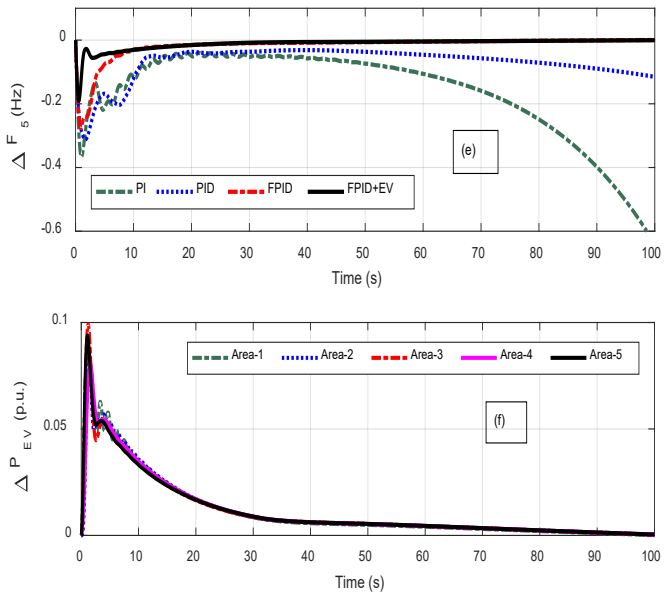

Fig. 9 System response for Case-4

6. Conclusions

A five-area nonlinear power system in presence of electric vehicle for frequency control of FPID based controller to optimize the parameters using hybridizing AVOA and PS (hAVOA-PS) is proposed in the system. The proposed hybrid AVOA-PS method takes the advantage of global search capability of AVOA and local search capability of PS algorithm. And also, the nonlinearities such as turbine dynamics, GRC and GDB are considered along with the electric vehicles and random load for the study of the effectiveness of the proposed work. Initially, a 5area ten-unit system without EV is assumed and the PI parameters are tuned by GA, PSO, AVOA and proposed hAVOA-PS methods. It is found that the % decrease in *ITAE* value with hAVOAO-PS method related to GA, PSO, and AVOA are 39.07%, 33.01% and 24.08%. In the next stage, PID, FPID controllers are considered and EVs are included in each area. It is noticed that, with the same hAVOAO-PStechnique, the % decrease in *ITAE* value with FPID with EVrelated to PI, PID, and FPID are 77.09%, 72.69% and 39.63% respectively. To exhibit the effectiveness of projected frequency control scheme, different cases like different SLI in all areas, different SLD in all areas, SLIs in some areas and SLDs in some areas as well as large SLIs in all areas. It is observed that the FPID with EV frequency control approach is able to preserve system stability for all the cases whereas PI and PID approaches fail to maintain stability in some cases. As a future study, the current work can be extended to a large system including unpredictable wind and solar energies. Also, the state of charge of EVs may be modelled and be taken into account for their participation in frequency control scheme.

References

[1] O. I. Elgerd and C. E. Fosha, "Optimum Megawatt-Frequency Control of Multiarea Electric Energy Systems," *IEEE Transactions on Power Apparatus and Systems,* 1970,vol. 89, no. 4, pp. 556 – 563.

[2] O. I. Elgerd and H. H. Happ, "Electric Energy Systems Theory: An Introduction," IEEE Transactions on Systems, Man, and Cybernetics,1972, Vols. SMC-2, no. 2, pp. 296-297.

[3] P. Kundur, "Power System Stability and Control," New Delhi: Tata McGraw, 2009.

[4] D. Das, S. K. Aditya and D. P. Kothari, "Dynamics of diesel and wind turbine generators on an isolated power system," International Journal of Electrical Power & Energy Systems,1999, vol. 21, no. 3, pp. 183-189.

[5] L. C. Saikia, J. Nanda and S. Mishra, "Performance comparison of several classical controllers in AGC for multi-area interconnected thermal system," International Journal of Electrical Power & Energy Systems,2011, vol. 33, no. 3, pp. 394-401.

[6] C. Ismayil, R. S. Kumar and T. K. Sindhu, "Optimal fractional order PID controller for automatic generation control of two-area power systems," International Transactions on Electrical Energy Systems, 2015, vol. 25, no. 12, pp. 3329-3348.

[7] L. C. Saikia, N. Sinha and J. Nanda, "Maiden application of bacterial foraging based fuzzy IDD controller in AGC of a multi-area hydrothermal system," International Journal of Electrical Power & Energy Systems,2013, vol. 45, no. 1, pp. 98-106.

[8] S. Mishra, R. C. Prusty and S. Panda, "Design and Analysis of 2dof-PID Controller for Frequency Regulation of Multi-Microgrid Using Hybrid Dragonfly and Pattern Search Algorithm," Journal of Control, Automation and Electrical Systems, 2020, vol. 31, p. 813–827.

[9] C. Wang, Y. Mi, Y. Fu and P. Wang, "Frequency Control of an Isolated Micro-Grid Using Double Sliding Mode Controllers and Disturbance Observer," IEEE Transactions on Smart Grid, 2018, vol. 9, no. 2, pp. 923 – 930.

[10] A. Kumar, R.K. Khadanga, S Panda, "Reinforced modified equilibrium optimization technique-based MS-PID frequency regulator for a hybrid power system with renewable energy sources " Soft Computing, 2021, https://doi.org/10.1007/s00500-021-06558-8

[11] H. Bevrani and P. Daneshmand, "Fuzzy logic-based load-frequency control concerning high penetration of wind turbines," IEEE systems journal,2012, vol. 6, no. 1, pp. 173-180.

[12] R.K. Khadanga, A Kumar and S Panda "A novel sine augmented scaled sine cosine algorithm for frequency control issues of a hybrid distributed two-area power system" Neural Computing and Applications 33 (19), 12791-12804

[13] P. Nayak, R. Prusty and S. Panda, "Grasshopper optimization algorithm optimized multistage controller for automatic generation control of a power system with FACTS devices," Protection and Control of Modern Power Systems, 2021,vol. 6, no. 8.

[14] P. C. Nayak, U. C. Prusty, R. C. Prusty and S. Panda, "Imperialist competitive algorithm optimized cascade controller for load frequency control of multi-microgrid system," Energy Sources, Part A: Recovery, Utilization, and Environmental Effects, 2021.

[15] P. C. Nayak, S. Mishra, R. C. Prusty and S. Panda, "Performance analysis of hydrogen aqua equalizer fuel-cell on AGC of Wind-hydro-thermal power systems with sunflower algorithm optimized fuzzy-PDFPI controller," International Journal of Ambient Energy,2020, vol. 43, pp. 1-14.

[16] P. C. Nayak, B. P. Nayak, R. C.Prusty and S. Panda, "Sunflower optimization based fractional order fuzzy PID controller," Energy Sources, Part A: Recovery, Utilization, and Environmental Effects, 2021,pp. 1-20.

[17] S. Abd-Elazim and E. Ali, "Load frequency controller design via BAT algorithm for nonlinear interconnected power system," International Journal of Electrical Power & Energy Systems,2016, vol. 77, pp. 166-177.

[18] S. K. Sinha, R. N. Patel and R. Prasad, "Application of GA and PSO Tuned Fuzzy Controller for AGC of Three Area Thermal- Thermal-Hydro Power System," International Journal of Computer Theory and Engineering, 2010, vol. 2, no. 2.

[19] P. C. Nayak, S. Patel, P. R. C. and P. S., "MVO-PS Optimized Hybrid FOFPID Controller for Load Frequency Control of an AC Micro-Grid System," International Journal of Recent Technology and Engineering (IJRTE),2019, vol. 8, no. 2, pp. 3805-3812.

[20] Y. Arya and N. Kumar, "BFOA-scaled fractional order fuzzy PID controller applied to AGC of multi-area multi-source electric power generating systems," Swarm and Evolutionary Computation, 2017, vol. 32, pp. 202-218.

[21] B. K. Sahu, S. Pati and S. Panda, "Hybrid differential evolution particle swarm optimisation optimised fuzzy proportional–integral derivative controller for automatic generation control of interconnected power system," IET Generation, Transmission & Distribution, 2014, vol. 8, no. 11, pp. 1789 - 1800.

[22] K. H. Ang, G. Chong and Y. Li, "PID control system analysis, design, and technology," IEEE Transactions on Control Systems Technology, 2005, vol. 13, no. 4, pp. 559-576.

[23] A. Demiroren and E. Yesil, "Automatic generation control with fuzzy logic controllers in the power system including SMES units," Electrical Power and Energy Systems, 2004, vol. 26, no. 4, pp.291–305.

[24] K. Parmar, S. Majhi and D. P. Kothari, "Improvement of Dynamic Performance of LFC of the Two Area Power System: an Analysis using MATLAB," International Journal of Computer Applications, 2012, vol. 40, no. 10.

[25] H.-X. Li and H. B. Gatland, "Conventional fuzzy control and its enhancement," in IEEE Transactions on Systems, Man, and Cybernetics, Part B (Cybernetics), 1996, vol. 26, no. 5, pp. 791-797.

[26] A. Fereidouni, M. A. Masoum and M. Moghbel, "A new adaptive configuration of PID type fuzzy logic controller," ISA Transactions, 2015, vol. 56, pp. 222-240.

[27] A. Savran and G. Kahraman, "A fuzzy model based adaptive PID controller design for nonlinear and uncertain processes," ISA Transactions, 2013, vol. 53, no. 2, pp. 280-288.

[28] A. E. Ezugwu, J. O. Agushaka, L. Abualigah, S. Mirjalili, A. H. Gandomi, "Prairie Dog Optimization Algorithm", Neural Computing and Applications, 2022,34:20017–20065

[29] J. O. Agushakaa, A. E. Ezugwua, L. Abualigah, Dwarf Mongoose Optimization Algorithm, Comput. Methods Appl. Mech. Engrg. 391 (2022) 114570

[30] J. O. Agushakaa, A. E. Ezugwua, L. Abualigah, Gazelle optimization algorithm: a novel nature-inspired metaheuristic optimizer, Neural Computing and Applications,2023,Vol. 35,pp.4099–4131

[31] G. Hu, Y. Zheng, L. Abualigah, A. G. Hussien, DETDO: An adaptive hybrid dandelion optimizer for engineering optimization, Advanced Engineering Informatics,2023, 57, 102004

[32] M. Zare, M. Ghasemi, A. Zahedi, K. Golalipour, S. K. Mohammadi, S. Mirjalili, L. Abualigah, A global best-guided firefly algorithm for engineering problems, *Journal of Bionic Engineering,*2023,Vol.20, pp.2359–2388.

[33] Guha D, Roy PK, Banerjee S, Quasi-oppositional JAYA optimized 2-degree-of-freedom PID controller for load-frequency control of interconnected power systems, Int. J. Simul. Model. 2020, vol.15,pp.1-23.

[34] Khokhar B, Dahiya S, Parmar KPS , Load frequency control of a microgrid employing a 2D Sine Logistic map based chaotic sine cosine algorithm, Applied Soft Computing,2021, Vol.109, 107564

[35] Peddakapu K, Mohameda MR, Srinivasarao P, Leung PK, Frequency stabilization in interconnected power system using bat and harmony search algorithm with coordinated controllers, Applied Soft Computing,2021, 113:107986

[36] El-Ela AAA, El-Sehiemy RA, Shaheen AM, Diab AE, Design of cascaded controller based on coyote optimizer for load frequency control in multi-area power systems with renewable sources, Control Engineering Practice,2022, vol.121, 105058

[37] Irudayaraj AXR, Wahab NIA, Premkumar M. et al. Renewable sources-based automatic load frequency control of interconnected systems using chaotic atom search optimization, Applied Soft Computing, doi: https://doi.org/10.1016/j.asoc.2022.108574,2022.

[38] Shayeghi H, Rahnama A, Alhelou HH, Frequency control of fully-renewable interconnected microgrid using fuzzy cascade controller with demand response program considering, Energy Reports,2021, Vol. 7,pp. 6077–6094

[39] Raj IAX, Wahab NIA, Umamaheswari MG et.al., A Matignon's Theorem Based Stability Analysis of Hybrid Power System for Automatic Load Frequency Control Using Atom Search Optimized FOPID Controller, IEEE Access. 2020, vol.8, pp. 168751-168772.

[40] Padhy S, Panda S , Application of a simplified Grey Wolf optimization technique for adaptive fuzzy PID controller design for frequency regulation of a distributed power generation system. Prot. Control Mod. Power Syst.2021, Vol.6, pp.1-6.

[41] B. Abdollahzadeh, F. S. Gharehchopogh, S. Mirjalili, African vultures optimization algorithm: A new nature-inspired metaheuristic algorithm for global optimization problems, Computers & Industrial Engineering,2021, 158, 107408

[42] B. Mohanty, S. Panda, and P. K. Hota, “Differential evolution algorithm based automatic generation control for interconnected power systems with non-linearity,” Alexandria Engineering J., 2014, vol. 53, pp. 537–552.
[43] K.R.M. Vijaya Chandrakala, S. Balamurugan, K. Sankaranarayanan, “Variable structure fuzzy gain scheduling-based load frequency controller for multi-source multi area hydro thermal system” Electrical Power and Energy Systems,2013, Vol. 53, pp. 375–381
[44] Pabitra Mohan Dash, Asini Kumar Baliarsingh, Sangram Keshori Mohapatra, Hybrid African Vulture Optimization Algorithm and Pattern Search Tuned Fractional Order PID Controller for AGC of Electric Vehicles Integrated Power Systems, International Journal on Electrical Engineering and Informatics,2023, Vol.15, Issue-2, pp.259-276,2023.